Molecular structure, vibrational spectroscopic (FT-IR, FT-Raman),UV-Vis spectra, first order hyperpolarizability, NBO analysis, HOMO and LUMO analysis, thermodynamic properties of 2,6-dichloropyrazine by ab inito HF and density functional method

M. V. S. Prasad, N. Udaya Sri, A. Veeraiah, V. Veeraiah,
and K. Chaitanya*

Molecular Spectroscopy Laboratories, Department of Physics, Andhra University, Visakhapatnam, India

Abstract. FT-IR and FT-Raman spectra of 2,6-dichloropyrazine were recorded and analyzed. The vibrational wavenumbers were examined theoretically using DFT/B3LYP /6-311G(d,p) level of theory. The data obtained from vibrational wavenumber calculations are used to assign vibrational bands obtained in infrared spectroscopy of the studied molecule. The calculated first hyperpolarizability is comparable with the reported values of similar derivatives and is an attractive object for future studies of nonlinear optics. The assignments of the vibrational spectra have been carried out with the help of normal co-ordinate analysis (NCA) following the Scaled Quantum Mechanical Force Field Methodology (SQMFF). UV-visible spectrum of the title molecule has also been calculated using TD-DFT/6-311G(d,p) method. The calculated energy and oscillator strength exactly reproduces reported experimental data. The Mulliken population analysis on atomic charges and the HOMO-LUMO energy are also calculated.

PACS: 31.15.E-, 31.15.ap, 33.20.Tp

Key words: 2, 6-dichloropyrazine, FT-IR, FT-Raman, UV-Vis, NBO, HOMO-LUMO

1   Introduction

Pyrazine and its derivatives are one of the most studied and important class of N-heterocycles. Pyrazines possess unique and extremely potent flavor and aroma characteristics [1,2]. Some of the derivatives of pyrazines find use as pharmaceutical intermediates[3],

---

*Corresponding author. *Email address:* cskcmail@gmail.com (K. Chaitanya)

marking volatiles[4], antifungal and antiviral agents[5] and hence they find extensive applications in flavor and pharmaceutical industries. alkyl-substituted pyrazine, is widely used as a key intermediate for pyrazineamide, an effective anti-tubercular drug [6,7].

Vibrational spectroscopy has been proven to be a useful probe of the structural properties of pyrazine.The pyrazines are the most extensively investigated class of diazines [8].Pyrazine (1,4-diazabenzene) is a diaza analogs of the benzene molecule. It is isoelectronic with benzene as it contain 6π electrons for aromatic delocalization. However, the perfect aromaticity of benzene is disturbed by centric substitution of 2 nitrogen atoms in the case of the systems under consideration, such that the electronegative nitrogens hold some of the ring electrons to prevent the perfect delocalization of the 6π electrons. The inclusion of a substituent group in aromatic rings leads to the variation of charge distribution in molecules, and consequently this greatly affects the structural, electronic and vibrational parameters. In general electron deficient pyrazines undergo electrophilic substitution reactions under normal conditions with the substitution of electron-donating group. That is the pyrazine system become more nucleophilic. Chlorine is generally referred to as highly electronegative and hence it withdraw the electrons from the ring which results in the change in ionization potential, electron affinity and excitation energies of the system.

Literature survey reveals that detailed interpretations of the infrared and Raman spectra have been reported on pyrazine [9-19] and dichloro substituted pyrazine [8]. For 2,6-dichloropyrazine the experimental results compared with the DFT/B3P86 method with 6-311G(d,p) basis set by assuming C$_{2v}$ symmetry. We have assumed C$_1$ symmetry for this molecule, because the molecule possesses minimum energy in this conformation [For C$_1$ symmetry , $E = -1183.6248893$ a.u. and C$_{2v}$ symmetry $E = -1183.62480348$ a.u.]. But the results based on density functional theory calculation with B3LYP/6-311G(d,p) and FT-IR, FT-Raman, UV-Vis spectral studies, the first order hyperpolarizabilities, the HOMO-LUMO and NBO analyses on 2,6-dichloropyrazine have no reports. This inadequacy in the literature encouraged us to make this theoretical and experimental vibrational spectroscopic research based on the structure on molecules to give a correct assignment of the fundamental bands in experimental FT-IR, FT-Raman spectra. Along with the vibrational spectra, the electronic potential should help us to understand the structural and spectral characteristic of this compound.

2   Experimental details

The compound 2,6-dichloropyrazine in the solid form was purchased from Sigma-Aldrich Chemical Company (USA) with a stated purity greater than 98% and it was used as such without further purification. Nicolet 6700 FT-IR spectrometer with an NXR FT-Raman module was used to record IR and Raman spectra. IR spectrum was recorded on samples dispersed in KBr pellets in the range of 400-4000 cm^{-1}. Raman spectrum was recorded on solid samples contained in standard NMR diameter tubes or on compressed samples con-

tained in a gold-coated sample holder. The FT-IR and FT-Raman spectra were recorded at Prof. Aswin Nangia's Lab, School of chemistry, University of Hyderabad. The ultraviolet absorption spectrum of 2,6-dichloropyrazine in solid form has been recorded in the range 200-500 nm using analytikjena SPECORD S-600, UV-Vis recording spectrometer at IISc., Bangalore.

3   Computational details

Quantum chemical density functional calculations using Becke's three-parameter(B3LYP) hybrid DFT level implemented with the standard 6-311G(d,p) basis set were carried out using Gaussian03W [20] to optimize the molecular geometry. The optimized geometry corresponding to the minimum on the potential energy surface has been obtained by solving self-consisting field equation iteratively. The harmonic vibrational frequencies have been analytically calculated by taking the second order derivative of energy using the same level of theory. The incompleteness of the basis set and vibrational anharmonicity consequences the overestimation of the computational frequencies. Therefore scaling of the force field was performed according to the scaled quantum mechanical procedure (SQM) [21,22] using selective scaling in the natural internal coordinate (see supplymentary material) representation [23,24] to obtain a better agreement between the theory and the experiment. Normal coordinate analysis has been performed in ordered to obtain the detailed interpretation of the fundamental modes using the MOLVIB program version7.0 written by Sundius [25, 26]. The vibrational frequencies are calculated by the MOLVIB with help of Gaussian force constants.

The Raman activities (S_i) calculated by the Gaussian'03W program are adjusted and converted in to relative raman intensities (I_i)during the scaling program with MOLVIB using the following relationship derived from the basic theory of Raman scattering[27,28]

$$I_i = f(v_0 - v_i)^4 S_i v_i^{-1} [1 - \exp(-hcv_i)/kT]^{-1} \tag{1}$$

where v_0 is the exciting frequency (in cm^{-1} units); v_i is the vibrational wave number of the ith normal mode; h,c,k are the universal constants and f is suitably chosen common normalization factor for all the intensities.

The NBO calculations [29] were performed using NBO 3.1 program as implemented in the Gaussian'03W package [20] at the DFT/B3LYP level in order to understand various second order interactions between the filled orbitals of one subsystem and vacant orbitals of another subsystem, which is a measure of delocalization or hyperconjugation. The second-order fock matrix was used to evaluate the donor-acceptor interactions in the NBO basis [30]. For each donor NBO(i) and acceptor NBO (j), the stabilization energy $E(2)$ associated with the i to j delocalization is estimated as

$$E(2) = \Delta E_{ij} = [q_i(F_{ij})^2]/[\varepsilon_i - \varepsilon_j] \tag{2}$$

where q_i is the ith donor orbital occupancy, $\varepsilon_i, \varepsilon_j$ are diagonal elements (orbital energies) and F_{ij} is the off diagonal element associated with NBO matrix.
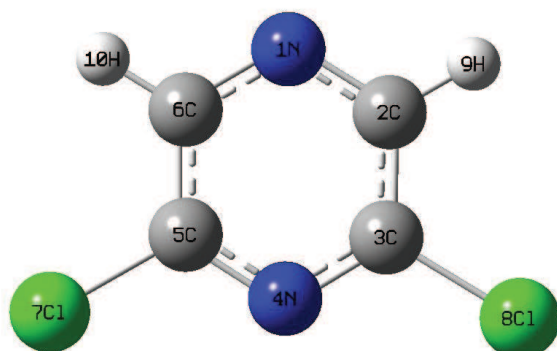
Figure 1: Molecular structures of 2, 6-dichloropyrazine along with numbering of atom.

4   Result and discussion

4.1   Geometry optimization

The molecular structure of the 2,6-dichloropyrazine belongs to C_1 point group symmetry. The optimized molecular structure of title molecule is shown in Fig. 1. The comparative optimized structural parameters such as bond lengths, bond angles and dihedral angles are presented in Table 1. From the theoretical values, it is found that most of the optimized bond lengths are slightly larger than the experimental values, due to that the theoretical calculations belong to isolated molecules in gaseous phase and the experimental results belong to molecules in solid state [31,32]. The pyrazine ring appears little distorted and angles slightly out of perfect hexagonal structure. It is due to the substitutions of the chlorine atom in the place of H atoms. The C-X (F, Cl, Br, etc.) bond length indicates a considerable increase when substituted in place of C-H. The optimized bond lengths of C-Cl are in good agreement with experimental results. The experimental value of C-Cl bond length is 1.7360 Å [31], 0.013 Å lesser than the calculated value (1.749 Å) by B3LYP/6-311G(d,p). The asymmetry of the pyrazine ring is evident by the bond angle order C2-N1-C6 , N1-C2-C3, C2-C3-N4, C3-N4-C5, N4-C5-C6 and N1-C6-C5. The bond angle N4-C5-C6 (cal. by B3LYP/6-311G(d,p) 122.7°) is ∼2° is greater than the bond angle N1-C6-C5 (cal. B3LYP/6-311G(d,p) 120.4°) due to the substitution of Cl atom. The calculated bond angle of C2-N1-C6 and C3-N4-C5 are 117.7 and 116.2 respectively, which is -0.1 and -1.6 differed from their experimental values [31]. The total energy obtained by the DFT structure optimization for the title compounds was found to be -1183.6248893 Hartrees.

4.2   Vibrational analysis

The symmetry of the title molecule is considered to be C_1. All the 24 vibrational normal modes of the molecule are IR and Raman active. The recorded FT-IR and FT-Raman

Table 1: Optimized geometrical parameters of 2,6-dichloropyrazine obtained by B3LYP/6-311G(d,p) density functional calculations.

Bond length (A°)[a]			Bond angle (°)[a]		
B3LYP/6-311G(d,p)	Exp[b]	Exp[c]	B3LYP/6-311G(d,p)	Exp[b]	Exp[c]
N1-C2	1.334	1.3473	1.315	C2-N1-C6	117.7	117.80	114.96
N1-C6	1.334	1.3205	1.327	N1-C2-C3	120.4	117.63	122.77
C2-C3	1.400	1.3803	1.355	N1-C2-H9	118.2	-	-
C2-H9	1.086	-	0.930	N1-C6-C5	120.4	124.55	121.68
C3-N4	1.324	1.3205	1.312	N1-C6-H10	118.2	-	119.20
C3-Cl8	1.749	1.7360	-	C3-C2-H9	121.5	-	-
N4-C5	1.324	1.3473	1.315	C2-C3-N4	122.7	124.55	122.76
C5-C6	1.400	1.3880	1.368	C2-C3-Cl8	119.7	119.25	-
C5-Cl7	1.749	1.7360	-	N4-C3-Cl8	117.7	116.18	-
C6-H10	1.086	-	0.930	C3-N4-C5	116.2	117.80	114.94
				N4-C5-C6	122.7	117.63	122.83
				N4-C5-Cl7	117.7	116.18	-
				C6-C5-Cl7	119.7	119.25	-
				C5-C6-H10	121.4	-	119.20

[a] For numbering of atoms refer to Fig. 1.
[b] See Ref. [31].
[c] See Ref. [32].

spectra for the compound in the solid phase can be seen in Figs. 2 and 3. The vibrational frequency obtained by density functional theory calculation is known for overestimation from the experimental values by 5% on average. An attempt was made to refine the scale factors using the set of transferable scale factors recommended by Rauhut and Pulay [33] are given in Table 2.The assignment of the experimental bands to the 24 expected normal vibration modes was made on the basis of the Potential Energy Distribution (PED) in terms of symmetry coordinates by using the B3LYP/6-311G(d,p) data and taking into account the previous assignment for the 2,6-dichloropyirazine [8] and pyrazine [9-19]. Table 3 shows the observed frequencies and the assignment of the vibrational normal modes. The theoretical calculations reproduce the normal wavenumbers by using the 6-311G(d,p) basis set, with an initial rms deviation value of 44.2 cm^{-1} while when the SQMFF method is applied the final value is 9.27 cm^{-1}.The complete description of the vibrational assignment is given below.

4.2.1 C-H vibrations

In general, the hetero aromatic organic compounds and its derivatives are structurally very close to benzene and commonly exhibit multiple peaks in the region 3100-3000 cm^{-1}. The CH stretching bands of pyrazine were reported in the range [8,19] 3100-3000

Table 2: Definition of local-symmetry coordinates and the values of corresponding scale factors used to correct the B3LYP/6-311G(d,p) (refined) force field of 2,6-dichloropyrazone.

No.(i)	Symbol[a]	Definition[b]	Scale factors
Stretching			
1-4	νNC	R_1, R_2, R_3, R_4	0.985
5-6	νCC	R_5, R_6	0.922
7-8	νCH	R_7, R_5	0.925
9-10	νCCl	R_9, R_{10}	0.920
In plane bending			
	βRtrid	$(\gamma_{11}-\gamma_{12}+\gamma_{13}-\gamma_{14}+\gamma_{15}-\gamma_{16})/\sqrt{6}$	0.910
11-13	βRsym	$(\gamma_{12}-\gamma_{13}+\gamma_{15}-\gamma_{16}/2$	0.950
	βRasy	$(2\gamma_{11}-\gamma_{12}-\gamma_{13}+2\gamma_{14}-\gamma_{15}-\gamma_{16})/\sqrt{12}$	0.970
14-15	βCH	$(\gamma_{17}-\gamma_{18})/2, (\gamma_{19}-\gamma_{20})/2,$	0.985
16-17	βCCl	$(\gamma_{21}-\gamma_{22})/2, (\gamma_{23}-\gamma_{24})/2,$	0.950
Out of plane bending			
18-19	ωCH	ω_{25}, ω_{26}	0.990
20-21	ωCCl	ω_{27}, ω_{28}	0.970
Torsion			
	τRtri	$(\tau_{29}-\tau_{30}+\tau_{31}-\tau_{32}+\tau_{33}-\tau_{34})/\sqrt{6}$	0.970
22-24	τRsym	$(\tau_{29}-\tau_{31}+\tau_{32}-\tau_{34})/2,$	0.970
	τRasy	$(-\tau_{29}+2\tau_{30}-\tau_{31}-\tau_{32}+2\tau_{33}-\tau_{34})/\sqrt{12}$	0.970

Abbreviations: ν, stretching; β, in plane bending; ω, out of plane bending; τ, torsion, tri, trigonal deformation, sym, symmetric deformation, asy, asymmetric deformation.
[a] These symbols are used for description of the normal modes by PED in Table 3.
[b] The internal coordinates used here are defined in supplementary material (Table 2-1).

Table 2-1: Supplementary material: definition of internal coordinates of 2,6-dichloropyrazine.

S.NO.	Symbol	Type	Definition
STRETCHING			
1 to 4	R_i	ν NC	N1-C2,C3-N4,N4-C5,C6-N1
5 to 6	R_i	νCC	C2-C3, C5-C6.
7 to 8	R_i	νCH	C6-H10, C2-H9.
9 to 10	R_i	νCCl	C5-Cl7, C3-Cl8.
IN PLANE BENDING			
11 to 16	β_i	Ring	N1-C2-C3, C2-C3-N4, C3-N4-C5, N4 -C5-C6, C5-C6-C1, C6-C1-C2,
17 to 20	β_i	CH	N1-C2-H9, C3- C2-H9, N1-C6-H10, C5-C6-H10.
21 to 24	β_i	CCl	C6-C5-Cl7, N4-C5-Cl7, C2-C3-Cl8, N4-C3-Cl8
OUT OF PLANE BENDING			
25 to 26	ω_i	CH	H9-C2-C3-N1, H10-C6-C5-N1.
27 to 28	ω_i	CCl	Cl7-C5-C6-N4, Cl8-C3-C2-N4.
29 to 34	τ_i	Ring	N1-C2-C3-N4, C2-C3-N4-C5, C3-N4-C5-C6, N4 -C5-C6-N1, C5-C6-N1-C2, C6-N1-C2-C3,
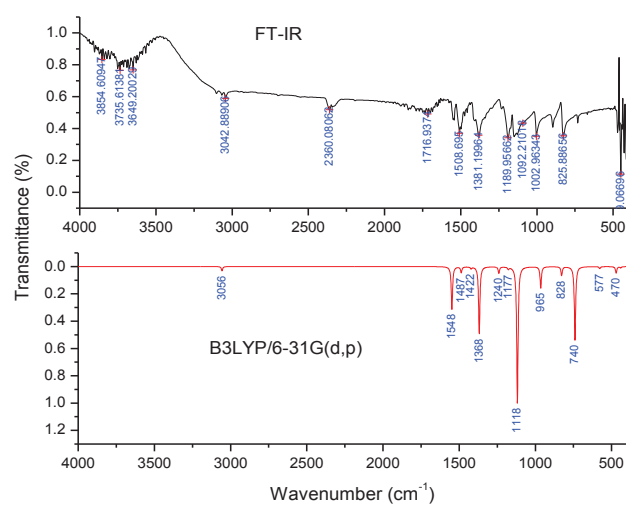
Figure 2: Experimental FT-IR spectra and simulated FT-IR spectra of 2,6-dichloropyrazine

cm^{-1}. The pyrazine CH stretching mode is observed at 3068(w) and 3040(ms) cm^{-1} in the IR spectrum and at 3045(ms) cm^{-1} in the Raman spectrum. B3LYP/6-311G(d,p) calculations give this mode at 3061 and 3056 cm^{-1}. CH stretching bands are observed at 3057, 3070, and 3086 cm^{-1} (IR); 3060, 3070, and 3087 cm^{-1} (Raman); and 3061, 3074, and 3079 cm^{-1} (theoretical) for 2-chloropyrazine; and at 3099 and 3104 cm^{-1} (IR); 3078 and 3103 cm^{-1} (Raman); and 3096 and 3100 cm^{-1} (calculated) for 2,6-dichloropyrazine[8]. Akyuz [34] reported these CH stretching bands at 3088, 3066, and 3052 cm^{-1} for pyrazinamide.The C-H out-of-plane bending vibrations occur in the region 900-667 cm^{-1} [8,19]. In this region the bands are not affected appreciable by the nature of the substituents. The IR bands observed at 1185ms and 1140(ms) cm^{-1} were assigned to C-H in-plane bending vibrations. The C-H out-of-plane bending modes were observed at 892 ans 821 cm^{-1} within the characteristic region and are presented in Table 3.

4.2.2   C-C vibrations

The bands between 1400 and 1650 cm^{-1} in the aromatic and hetero aromatic compounds are assigned to carbon vibrations [35]. The actual positions are determined not by the nature of the substituent's but rather by the form of the substitution around the aromatic ring. Moreover when C-N or more double modes are in conjugation the delocalization of electrons result in a transfer of some bond order to intervening single bonds are hence, there is full in the carbon-carbon stretching frequency. In the present study the FTIR bands observed at 1467, 998 cm^{-1} and Raman bands observed at 1004 cm^{-1} have been assigned to carbon-carbon stretching vibration[8,19]. The frequencies observed in FT-Raman spectrum at 950 ,572 cm^{-1} and 657, 476 cm^{-1} have been assigned to C-C in-plane and out-of-plane bending vibrations.
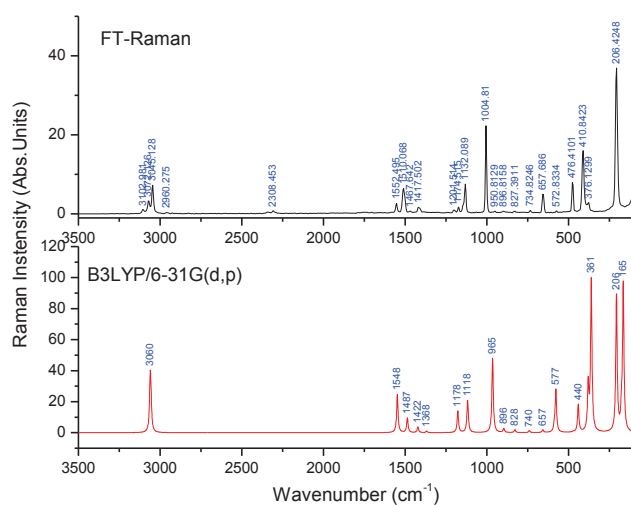
Figure 3: Experimental FT-Raman spectra and simulated FT-Raman spectra of 2,6-dichloropyrazine.

4.2.3   C=N and C-N vibrations

The identification of C-N and C=N vibrations are a very difficult task, since the mixing of several modes are possible in the region. Silverstein *et al.* [36] assigned C-N stretching absorption in the region 1266-1382cm^{-1} for aromatic amines. In pyrazine, the C-N stretching bands are found to be present at 1307 and 1382 cm^{-1} [8,19]. In the present work, the bands observed at 1548(s), 1379, 1185 and 1140 cm^{-1} in FT-IR spectrum have been assigned to C=N and C-N stretching vibrations, respectively. The same vibration which corresponds to Raman spectrum is at 1417(vw) and 1174(w) cm^{-1} . The theoretically computed values of C=N and C-N stretching vibrations also fall in the regions of 1548, 1422, 1240 and 1178 cm^{-1} . The DFT method is in agreement with experimental data.

4.2.4   C-Cl vibrations

Involving the ring-halogen modes is related partially to Cl-C stretching and bending modes. These modes are in 200-600 cm^{-1} frequency range as reported by Endredi *et al.* [8]. The band 729(vw),441(w) cm^{-1} in FT-IR and 734(vw) , 410(s) cm^{-1} in FTRaman are assigned to the C-Cl stretching mode According to the calculated PED, our calculations show that there is no pure C-Cl band in this range. The C-Cl in-plane bending modes are located at 385(vs) in FT-IR and 206(vs) cm^{-1} in FT-Raman spectra[8]. The C-Cl out-of-plane bending modes are assigned to calculated values 361 and 176 cm-1 as shown in Table 3.

Table 3: Detailed assignments of fundamental vibrations of 2,6-dichloropyrizine by normal mode analysis based on SQM force field calculations using 3LYP/6-311G (d,p).

No.	Experimental (cm^{-1})		Scaled frequencies(cm^{-1})	Intensity		Characterization of normal modes with PED (%)^d
	FT-IR	FT-Raman		I_{IR}^b	I_{RA}^c	
1	3068w		3061	0.016	39.10	νCH(99)
2	3040ms	3045ms	3056	0.032	32.10	νCH(99)
3	1548s		1548	0.314	24.60	νNC(88)
4	1467vw		1486	0.047	9.70	νCC(33), νNC(33), βCH(27)
5	1379s	1417vw	1422	0.019	3.78	νNC(56), βCH(23), βCCl(11)
6			1368	0.493	1.06	βCH (60), νNC(29)
7	1185ms		1240	0.050	0.17	νNC (70), βCH(23)
8	1140ms	1174w	1178	0.024	14.10	νNC (53), βCH(42)
9			1119	0.968	19.80	νCC (57), νCCl(14), νNC(14)
10	998s	1004vs	1117	0.967	20.80	νCC (42), νCCl(21), νNC(16), Rtri(11)
11		950vw	965	0.159	48.10	Rtri(67), νNC (17), νCC (11)
12	892ms	896vw	896	0.002	2.86	ωCH (91)
13	821s	827vw	828	0.068	1.95	ωCH (91)
14	729vw	734vw	740	0.540	1.35	νCCl(57), Rasy(24), Rsym (14)
15		657ms	657	0.002	2.01	τRtri (66), ωCCl(28)
16			587	0.004	9.47	Rsym (67), τRsym(23)
17		572vw	577	0.015	28.30	Rsym (38), νCCl(21), Rasyd(18)
18	480w	476ms	470	0.049	1.31	τRasy (48), ωCCl(22), ωCH (16), τRsym(13)
19	441	410s	440	0.010	18.50	βCCl(46), Rasy(27), νCCl(18)
20	385vs	376w	380	0.007	35.90	βCCl(58), νCCl(18), Rsym (10)
21	349w		361	0.010	100.00	ωCCl(38), Rasy(29), Rsym (23)
22		206vs	206	0.000	89.60	βCCl(79)
23			176	0.000	29.20	ωCCl(59), τRtri(18), τRasy (13)
24			165	0.000	97.80	τRsym (62), τRasy(25)

^{a} Abbreviations: ν, stretching; β, in plane bending; ω, out of plane bending; τ, torsion; tri, trigonal deformation, sym, symmetrical deformation, asy, asymmetric deformation, vs, very strong; s, strong; ms, medium strong; w, weak; vw, very weak.
^{b} Relative absorption intensities normalized with highest peak absorption equal to 1.
^{c} Relative Raman intensities calculated by Eq. (1) and normalized to 100.
^{d} Only PED contributions $\geq$10% are listed.

5   Polarizability and hyperpolarizability

Analysis of organic molecules having conjugated π-electron systems and large hyperpolarizability using infrared and Raman spectroscopy has been evolved as a subject of research [37]. The polarizabilities and hyperpolarizabilities characterize the response of a system inan applied electric field [38,39]. In the presence of an electric field, the energy of a system is a function of the electric field. The first hyperpolarizability is a third-rank tensor that can be described to 10 components by a 3x3x3 matrix due to Kleinmen symmetry [40,41]. In the present study, the second-order polarizability or first hyperpolarizability β, dipole moment μ and polarizability α was calculated using HF/6-311G(d,p) basis set on the basis of the finite-field approach. The complete equations for calculating the magnitude of total static dipole moment μ, the mean polarizability α_0, the anisotropy of the polarizability $\Delta\alpha$ and the mean first hyperpolarizability β_0, using the x,y,z components
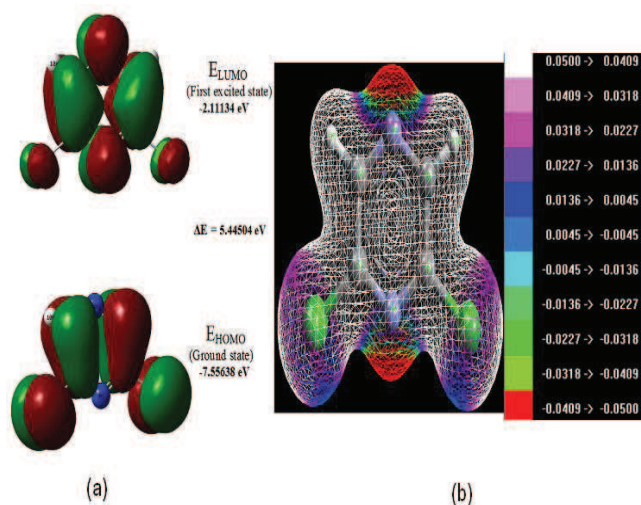
Figure 4: (a)The atomic orbital components of the frontier molecular orbital and (b) molecular electrostatic potential surface of 2,6-dichloropyrazine.

are given by following equations

$$E = E^0 - \mu \alpha F_\alpha \frac{1}{2} \alpha_0 \beta F_\alpha F_\beta - \frac{1}{6} \beta_{\alpha \beta y} F_\alpha \alpha F_\beta F_y + \cdots \tag{3}$$

where E_0 is the energy of the unperturbed molecules, F_α is the field at the origin and $\mu\alpha$, $\alpha_{\alpha\beta}$, and $\beta_{\alpha\beta\gamma}$ are the components of dipole moment, polarizability and the first hyperpolarizabilities, respectively. The total static dipole moment μ, the mean polarizability α_0, the anisotropy of the polarizability $\Delta\alpha$ and the mean first hyperpolarizability β_0, using the x, y, z components they are defined as

$$\mu = (\mu_x^2 + \mu_y^2 + \mu_z^2)^{1/2} \tag{4}$$

$$\alpha_0 = [\alpha_{xx} + \alpha_{yy} + \alpha_{zz}]/2 \tag{5}$$

$$\Delta\alpha = 2^{-1/2}[(\alpha_{xx} - \alpha_{yy})^2 + (\alpha_{yy} - \alpha_{zz})^2 + (\alpha_{zz} - \alpha_{xx})^2 + 6\alpha_{xx}^2]^{1/2} \tag{6}$$

$$\beta_0 = (\beta_x + \beta_y + \beta_z)^{1/2} \tag{7}$$

$$\beta_x = \beta_{xxx} + \beta_{xyy} + \beta_{xyz} \tag{8}$$

$$\beta_y = \beta_{yyy} + \beta_{xxz} + \beta_{yyz} \tag{9}$$

$$\beta_z = \beta_{zzz} + \beta_{xxz} + \beta_{yyz} \tag{10}$$

The HF/6-311G(d) calculated first hyperpolarizability of 2,6-dichloropyrazine 1.0048 84×10^{-30} esu and the dipole moment is 0.5625 Debye are shown in Table 4. The calculated first hyperpolarizability of 2,6-dichloropyrazine is about 14 times greater than that of urea. The above results show that title compound is best material for NLO applications.

Table 4: The electric dipole moment μ (D), the average polarizability $\alpha_{tot}(\times 10^{-24}$ esu) and the first hyperpolarizability $\beta_{tot}(\times 10^{-30}$ esu) of 2,6-dichloropyrazine by HF/6-311G(d, p) method.

μ and α components	2, 6-dichloropyrazine	β components	2, 6-dichloropyrazine
μ_x	-0.4895107	β_{xxx}	-75.0193478
μ_y	0.00014	β_{xxy}	0.0191188
μ_z	-0.2772139	β_{xyy}	0.6205513
μ_{tot}(D)	0.562555	β_{yyy}	-0.0027278
α_{xx}	83.378041	β_{xxz}	39.4750013
α_{xy}	-0.0324628	β_{xyz}	-0.0106901
α_{yy}	29.7898326	β_{yyz}	0.3512861
α_{xz}	-16.8010123	β_{xzz}	-26.8188751
α_{yz}	0.031415	β_{yzz}	0.0093349
α_{zz}	103.538683	β_{zzz}	-97.1347915
α_{tot}(esu)	158.7898 x10-24	β_{total} (esu)	1.004884×10^{-30}

6   NBO analysis

NBO analysis has been performed on the molecule at the DFT/B3LYP/6-311G(d, p) level in order to elucidate the intra molecular, rehybridization and delocalization of electron density within the molecule. The intramolecular interactions are formed by the orbital overlap between bonding (C-C), (N-C) and (C-C, (N-C) anti bonding orbital which results intramolecular charge transfer (ICT) causing stabilization of the system.

These interactions are observed as increase in electron density (ED) in C-C, C-N anti bonding orbital that weakens the respective bonds. The electron density of conjugated double as well as single bond of the aromatic ring (1.9e) clearly demonstrates strong delocalization inside the molecule. The strong intramolecular hyperconjugation interaction of the σ and π electrons of N-C to the anti N-C bond in the ring leads to stabilization of some part of the ring as evident from Table 5. The intramolecular hyper conjugative interaction of the N1-C6 distribute to C5-C7 leading to stabilization of 3.62 kJ/mol. This enhanced further conjugate with anti bonding orbital of π^* C2-C3, and N4-C5 leads to strong delocalization of 22.83, and 20.06 kJ/mol respectively. The same kind of interaction is calculated in the same kind of interaction energy, related to the resonance in the molecule, is electron donating from n_1(Cl17) and n_2(Cl17) to the π^*(N4-C5) show less stabilization of 1.08 and 6.88 kJ/mol respectively and further n3(Cl17) conjugate with π^*(N4-C5) through antibond, i.e. π^*(C1-C2) leads to the strong stabilization energy of 16.75 kJ/mol.Similary in the case of lone pair n_1(Cl18) , n_2(Cl18) and n_3(Cl18). The π^*(N4-C5) of the NBO conjugated with π^* (N1-C6) and (C2-C3) resulting a strong stabilization energy 182.38 and 99.48 kJ/mol respectively.These results indicating the strong intramolecular hypercon-

Table 5: Second order perturbation theory analysis of fock matrix in NBO basis for 2,6-dichloropyrazine.

Donor(*i*)	Type	ED/e	Acceptor(*j*)	Type	ED/e	$E(2)^a$ (Kj mol^{-1})	$E(j) - E(i)^b$ (a.u.)	$F(i,j)^c$ (a.u.)
N1 - C2	σ	1.98208	C3 -Cl8	σ^*	0.05911	3.62	0.95	0.053
N1 - C6	σ	1.98209	C5 -Cl7	σ *	0.05905	3.62	0.95	0.053
N1 - C6	π	1.69811	C2 - C3	π^*	0.34051	22.83	0.30	0.075
			N4 - C5	π^*	0.43825	20.06	0.27	0.068
C2 - C3	π	1.60881	N1 - C6	π^*	0.35777	18.35	0.27	0.064
			N4 - C5	π^*	0.43825	20.96	0.25	0.066
N4 - C5		1.71883	N1 - C6	π^*	0.35777	17.44	0.31	0.067
			C2 - C3	π^*	0.34051	20.04	0.31	0.072
C5 -Cl7	σ	1.98885	C3 - N4	σ^*	0.03326	2.82	1.20	0.052
N1	n1	1.91311	C2 - C3	σ^*	0.04466	9.14	0.88	0.081
			C5 - C6	σ^*	0.04467	9.15	0.88	0.081
N4	n1	1.89238	C2 - C3	σ^*	0.04466	8.60	0.87	0.079
			C5 - C6	σ^*	0.04467	8.59	0.87	0.079
Cl7	n1	1.99354	N4 - C5	σ^*	0.03328	1.08	1.39	0.035
			C5 - C6	σ^*	0.04467	1.51	1.44	0.042
Cl7	n2	1.96176	N4 - C5	σ *	0.03328	6.88	0.79	0.066
			C5 - C6	σ *	0.04467	3.65	0.84	0.050
Cl7	n3	1.91030	N4 - C5	π^*	0.43825	16.75	0.28	0.068
Cl8	n1	1.99354	C2 - C3	σ *	0.04466	1.51	1.44	0.042
Cl8	n2	1.96178	C2 - C3	σ^*	0.04466	3.65	0.84	0.050
			C3 - N4	σ^*	0.03326	6.87	0.79	0.066
Cl8	n3	1.91034	C2 - C3	π^*	0.34051	13.89	0.31	0.063
N4 - C5	π^*	0.43825	N1 - C6	π^*	0.35777	182.38	0.02	0.087
			C2 - C3	π^*	0.34051	99.48	0.03	0.075

[a] *E*(2) means energy of hyper conjugative interaction (stabilization energy).
[b] Energy difference between donor and acceptor *i* and *j* NBO orbitals.
[c] *F*(*i*,*j*) is the Fock matrix element between *i* and *j* NBO orbitals.

jugative interaction within the molecule and stability of the molecule.

7   Electronic absorption spectra

Both the highest occupied molecular orbital (HOMO) and lowest unoccupied molecular orbital (LUMO) are the main orbitals take part in chemical stability [42]. The HOMO represents the ability to donate an electron, LUMO as an electron acceptor represents the ability to obtain an electron. The HOMO and LUMO energy calculated by B3LYP/6-311G(d,p) method are given in Table 6. The 3D plots of the frontier orbitals HOMO and LUMO and the molecular electrostatic potential map (MEP) for both the molecules are shown in Fig. 4. It can be seen that from the Fig. 4(a), the HOMO is located over chlorine and carbon atoms; the HOMO-LUMO transition implies an electron density transfer to chlorine to nitrogen atoms in the ring. The HOMO-LUMO energy gap of 2,6-
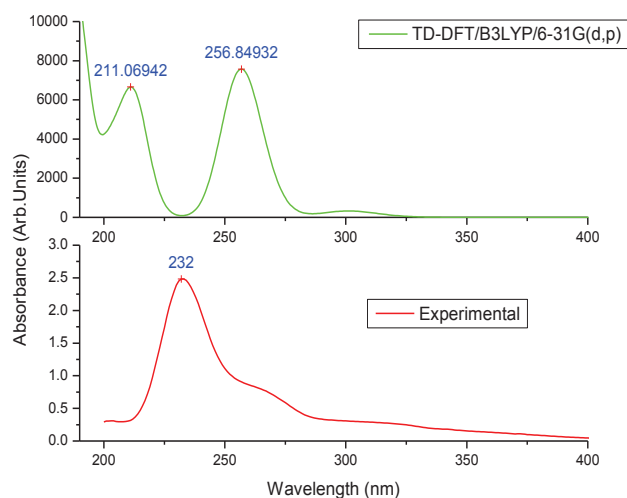
Figure 5: UV-visible spectra of 2,6-dichloropyrazine.

Table 6: The Total energy and frontier molecular orbital energies of 2,6-dichloropyrazine obtained by using B3LYP/6-311G(d,p).

Property	2,6-dichloropyrazine
Total energy (a.u.)	-1183.6248893
E_{HOMO} (eV)	-7.556389204
E_{LUMO} (eV)	-2.111348044
$\Delta E = E_{HOMO} - E_{LUMO}$ (eV)	5.445041160

dichloropyrazine calculated at the DFT/B3LYP method with 6-311G(d,p) level is shown in Table 6 and it reveals that the energy gap reflect the chemical activity of the molecule. LUMO as an electron acceptor represents the ability to accept an electron and HOMO represents the ability to donate an electron. Molecular electrostatic potential (MEP) mapping is very useful in the investigation of the molecular structure with its physiochemical property relationships [43-48]. Being a real physical property, $V(r)$ can be determined experimentally by diffraction or by computational methods. To predict reactive sites for electrophilic and nucleophilic attack for the investigated molecule, the MEP at the B3LYP/6-311G(d) optimized geometry was calculated. The negative (red and yellow) regions of the MEP are related to electrophilic reactivity and the positive (blue) regions to nucleophilic reactivity, as shown in Fig. 4(b).

All the structures allows strong $\pi \rightarrow \pi^*$ or $\pi \rightarrow \pi^*$ transition in the UV-vis region with high extinction coefficients. Natural bond orbital analysis indicates that molecular orbitals are mainly composed of σ and π atomic orbital. The UV-vis absorption spectrum of the sample in solid form is shown in Fig. 5. On the basis of fully optimized ground-state structure, TD-DFT/B3LYP/6-311G(d,p) calculations have been used to determine the

low-lying excited states of 2,6-dichloropyrazine. The calculated results involving the vertical excitation energies, oscillator strength (f) and wavelength are carried out and compared with measured experimental wavelength. Typically, according to Frank-Condon principle, the maximum absorption peak (λ_{max}) correspond in UV-vis spectrum to vertical excitation TD-DFT/B3LYP/6-311G(d,p) predict one intense electronic transition at 256.84 nm with an oscillator strength $f = 0.1046$, shows good agreement with measured experimental data ($\lambda_{exp} = 232$ nm). Both the highest occupied molecular orbital (HOMO) and lowest unoccupied molecular orbital (LUMO) are the main orbitals that take part in chemical stability [49]. Table 7 shows the electronic absorption wave lengths and oscillator strengths calculated by TDDFT/6-311G(d,p) along with experimental values.

The ionization potential of the pyrazine is 8.85 eV [50]. The ionisation potential calculated for 2,6-dichloropyrazine (7.556 eV) have lower potential than that of pyrazine. The effect of substitution of chlorine on pyrazole decreases the ionisation potential of the 2,6-dichloropyrazine. Considering the chemical hardness, large HOMO-LUMO gap means a hard molecule and small HOMO-LUMO gap means a soft molecule. One can also relate the stability of the molecule to hardness, which means that the molecule with least HOMO-LUMO gap means it is more reactive.

Table 7: The UV-vis excitation energy and oscillator strength for 2,6-dichloropyrazine calculated by TDDFT/B3LYP/6-311G(d,p) method.

S.no	Exp. (nm)	Energy (cm)$^{-1}$	Wavelength (nm)	Osc Strength	Symmetry	Major contribs
1		33232.69	300.90	0.0045	Singlet-A	H-1->LUMO (93%)
2		38785.05	257.83	0.0	Singlet-A	H-1->L+1 (99%)
3	232	38968.94	256.61	0.1046	Singlet-A	HOMO->LUMO (81%)
4		41563.64	240.59	0.0001	Singlet-A	H-2->LUMO (91%)
5		47120.04	212.22	0.0833	Singlet-A	H-3->LUMO (23%), HOMO -> L+1 (60%)
6		47958.86	208.51	0.0	Singlet-A	H-2->L+1 (97%)
7		48624.27	205.65	0.0	Singlet-A	H-4->LUMO (99%)
8		49564.72	201.75	0.0451	Singlet-A	H-6->LUMO (-12%), H-3->LUMO (58%)
9		51441.59	194.39	0.0003	Singlet-A	H-5->LUMO (92%)
10		52945.01	188.87	0.0	Singlet-A	HOMO->L+2 (95%)

8 Thermodynamic properties

On the basis of vibrational analyses and statistical thermodynamics, the standard thermodynamic functions: heat capacity, internal energy, entropy and enthalpy were calculated using Moltran v.2.5 [51] and are listed in Table 8. As observed from Table 8, the values of C_P, C_V, U, H and S all increase with the increase of temperature from 100 to 500 K, which is attributed to the enhancement of the molecular vibration as the temperature increases. The correlation equations between these thermodynamic properties and temperatures were fitted by quadratic, linear and quadratic formulas, respectively, and the

Table 8: Thermodynamic properties for the 2,6-dichloropyrazine obtained by B3LYP/6-311G(d,p) density functional calculations.

| Temperature | C_V | C_P | U | H | S | G |
K	J/K/mol	J/K/mol	KJ/mol	KJ/mol	J/K/mol	KJ/mol
100.000	42.651	50.965	153.134	153.965	260.489	127.916
200.000	70.140	78.454	158.778	160.441	304.285	99.584
300.000	96.414	104.728	167.122	169.617	341.128	67.278
400.000	119.635	127.949	177.958	181.284	374.533	31.471
500.000	138.481	146.796	190.902	195.059	405.192	-7.537
$C_v = 10.9482 + 0.32832\ T - 1.45279 \times 10^{-4}\ T^2$						
$C_p = 19.2628 + 0.32832\ T - 1.45264 \times 10^{-4}\ T^2$						
$U = 149.710 - 0.02146\ T + 1.22086 \times 10^{-4}\ T^2$						
$H = 149.7084 + 0.02979\ T + 1.22064 \times 10^{-4}\ T^2$						
$S = 214.3732 + 0.48699\ T - 2,12229 \times 10^{-4}\ T^2$						
$G = 153.0216 - 0.23251\ T - 1.7752 \times 10^{-4}\ T^2$						

corresponding fitting equations are also listed in Table 8 and the corresponding fitting factors are all beyond 0.999.

All the thermodynamic data provide helpful information to further study on the title compounds. They computes the other thermodynamic energies according to relationships of thermodynamic functions and estimate directions of chemical reactions according to the second lawof thermodynamics in thermochemical field.All thermodynamic calculations were done in gas phase and they could not be used in solution. Dipole moment reflects the molecular charge distribution and is given as a vector in three dimensions. Therefore, it can be used as illustrator to depict the charge movement across the molecule. Direction of the dipole moment vector in a molecule depends on the centres of negative and positive charges. Dipole moments are strictly identified for neutral molecules. For charged systems, its value depends on the choice of origin and molecular orientation.

9　Conclusions

In this paper we have reported complete structural, vibrational and electronic properties of the title compound by using experimental techniques (FT-IR, FT-Raman and UV-Vis absorption spectra) and theoretical method (DFT/B3LYP/6-311G(d,p)).The scaled vibrational frequencies are in good agreement with the experimental data. The vibrational modes of the experimental wavenumbers are assigned on the basis of potential energy distribution (PED). The calculated first hyperpolarizability of 2,6-dichloropyrazine is about 14 times greater than that of urea. The above results show that title compound is best material for NLO applications. NBO analysis indicating the strong intramolec-

ular hyperconjugative interaction within the molecule and stability of the molecule. In the UV-vis absorption spectrum one intense electronic transition $\pi \to \pi^*$ is observed at $\lambda_{\max} = 232$ nm.

References

[1] J. T. Andrew and D. S. Mottaram, Flavor Science: Recent Developments (Woodhead Publishing, Great Britain, 1996), p. 202.

[2] O. R. Fennema, Food Chemistry (Marcel Dekker, The Ohio State Univer., Colombus, Ohio, 1996), p. 741.

[3] D. J. Brown, The Pyrazines (John-Wiley Interscienc, New York, 2002), p. 77.

[4] A. K. Borg-Karlso and J. J. Tengo, Chem. Ecology 6 (1980) 827.

[5] J. A. Joule and K. Mills, Heterocyclic Chemistry (Wiley-Blackwell, New York, 2002) p.194.

[6] S. P. Seetharamanjaneya, K. V. Raghavan, P. K. Rao, and S. J. Kulkarni, 2002 US 143180 A1.

[7] L. Forni, G. Stern, and M. Gatti, Appl. Catal. 29 (1987) 161.

[8] H. Endredi, F. Billes, S. Holly, J. Mol. Struct. (Theochem.) 633 (2003) 73.

[9] P. J. Chappell and I.G. Ross, Chem. Phys. Lett. 43 (1976) 440.

[10] K. B. Wiberg, J. Mol. Struct. 224 (1990) 61.

[11] F. Billes and H. Mikosch, Acta Chim. Hung. 130 (1993) 901.

[12] F. Billes, H. Mikosch, and S. Holly, J. Mol. Struct. (Theochem.) 423 (1998) 225.

[13] J. M. L. Martin and C. Van Alsenoy, J. Phys. Chem. 100 (1996) 6973.

[14] A. D. Boese and J. M. L. Martin, J. Phys. Chem. A 108 (2004) 3085.

[15] D. B. Scully, Spectrochim. Acta 17 (1961) 233.

[16] M. A. Montan?ez, I. L. Toco?n, J. C. Otero, and J. I. Marcos, J. Mol. Struct. 482 (1999) 201.

[17]] J. F. Arenas, J. T. Lopez Navarrete, J. C. Otero, and J. I. Marcos, Faraday Trans. 81 (1985) 405.

[18] G. J. Kearley, J. Tomkinson, A. Navarro, J. J. L. Gonzalez, and M. F. Gomez, Chem. Phys. 216 (1997) 216.

[19] S. Breda, I. D. Reva , L. Lapinski , M.J. Nowak, and R. Fausto, J. Mol. Struct. 786 (2006) 193.

[20] M. J. Frisch, G. W. Trucks, H. B. Schlegel, *et al.*, Gaussian 03, Rev. D.1 (Gaussian, Inc., Pittsburgh, PA, 2005).

[21] G. Rauhut and P. Pulay, J. Phys. Chem. 99 (1995) 3093.

[22] P. Pulay, G. Fogarasi, G. Pongor, J. E. Boggs, and A. Vargha, J. Am. Chem. Soc. 105 (1983) 7037.

[23] G. Fogarasi, P. Pulay, J. R. Durig, Vibrational Spectra and Structure, Vol. 14 (Elsevier, Amsterdam, 1985).

[24] G. Fogarasi, X. Zhov, P. W. Taylor, and P. Pulay, J. Am. Chem. Soc. 114 (1992) 8191.

[25] T. Sundius, J. Mol. Struct. 218 (1990) 321.

[26] T. Sundius, Vib. Spectrosc. 29 (2002) 89.

[27] G. Keresztury, S. Holly, J. Varga, G. Besenyei, A. Y. Wang, and J. R. Durig, Spectrochim. Acta A 49 (1993) 2007.

[28] J. M Chalmers and P. R. Griffith, Raman Spectroscopy: Theory in Handbook of Vibrational Spectroscopy, Vol. 1 (John Wiley & Sons Ltd., New York, 2002), p. 71.

[29] E. D. Glendening, A. E. Reed, J. E. Carpenter, and F. Weinhold, NBO Version 3.1 (TCI, University of Wisconsin, Madison, 1998).

[30] A. E. Reed, L. A. Curtiss, and F. Weinhold, Chem. Rev. 88 (1988) 899.

[31] T. M. Barby, A. W. Corder, R. T. Oakley, K. E. Preuss, and H. Zang, Acta. Cryst. C 54 (1998) 1018.

[32] C. H. Zhang, X. J. Tan, and D. X. Xing, Acta. Cryst. E 65 (2009) 2902.

[33] P. Pulay, G. Fogarasi, F. Pong, and J. E. Boggs, J. Am. Chem. Soc. 101 (1979) 2550.

[34] S. Akyuz, J. Mol. Struct. 651 (2003) 541; S. Akyuz, J. Mol. Struct. 651 (2003) 541.

[35] G. Varsanyi, Vibrational Spectra of Seven Hundred Benzene Derivatives (Academic Press, New York, 1969).

[36] M. Silverstein, G. C.Basseler, and C. Morill, Spectrometric Identification of Orgganic Compound (Wiely, New York, 1981).

[37] M. Tommasini, C. Castiglioni, M. Del Zoppo, and G. Zerbi, J. Mol. Struct. 480 (1999) 179.

[38] C. R. Zhang, H. S. Chem, and G. H. Wang, Chem. Res. Chin. Univ. 20 (2004) 640.

[39] P. S. Kumar, K. Vasudevan, A. Prakasam, M. Geetha, and P.M. Anbarasan, Spectrochim. Acta A 77 (2010) 45.

[40] D. A. Kleinman, Phys. Rev. 126 (1962) 1977.

[41] J. Karparm, N. Sundaraganesan, S. Sebastian, S. Manoharan, and M. Kurt, J. Raman. Spectrosc. 41 (2010) 53.

[42] S. Gunasekaran, R. A. Balaji, S. Kumaresan, G. Anand, and S. Srinivasan, Can. J. Anal. Sci. Spectrosc. 53 (2008) 149.

[43] J. S. Murray and K. Sen, Molecular Electrostatic Potentials, Concepts and Applications (Elsevier, Amsterdam, 1996).

[44] I. Alkorta and J. J. Perez, Int. J. Quant. Chem. 57 (1996) 123.

[45] P. Lowdin, Advances in Quantum Chemistry (Academic Press, New York, 1978).

[46] F. J. Luque, M. Orozco, P. K. Bhadane, and S. R. Gadre, J. Phys. Chem. 97 (1993) 9380.

[47] J. Sponer and P. Hobza, Int. J. Quant. Chem. 57 (1996) 959.

[48] P. M. Anbarasana, M. K. Subramanian, P. Senthilkumar, C. Mohanasundaram, V. Ilangovan, and N. Sundaraganesan, J. Chem. Pharm. Res. 3 (2011) 597.

[49] S. Gunasekaran, R. S. Balaji, S. Kumaresan, G. Anand, and S. Srinivasan, Can. J. Anal. Sci. Spectrosc. 53 (2008) 149.

[50] E. Haselbach, Z. Lanyiova, and M. Rossi, Helv. Chim. Acta 56 (1973) 2889.

[51] S. K. Ignatov, Moltran V.2.5: Program for Molecular Visualization and Thermodynamic Calculations (University of Nizhny, Novgorod, 2004). http://ichem.unn.ru/Moltran.